Received: 16 June 2021 | Accepted: 29 July 2021

DOI: 10.1002/iub.2541

SPECIAL ISSUE

IUBMB LIFE WILEY

Impact of natural mutations on the riboflavin transporter 2 and their relevance to human riboflavin transporter deficiency 2

Lara Console[1] | **Maria Tolomeo**[2] | **Jessica Cosco**[1] | **Keith Massey**[3] | **Maria Barile**[2] | **Cesare Indiveri**[1]

[1]Department DiBEST (Biologia, Ecologia, Scienze della Terra) Unit of Biochemistry and Molecular Biotechnology, University of Calabria, Arcavacata di Rende, Italy

[2]Department of Biosciences, Biotechnology, and Biopharmaceutics, University of Bari, Bari, Italy

[3]Cure RTD Foundation, Calgary, Alberta, Canada

Correspondence
Maria Barile, Department of Biosciences, Biotechnology, and Biopharmaceutics, University of Bari, via Orabona 4 – 70126 Bari, Italy.
Email: maria.barile@uniba.it

Cesare Indiveri, Department DiBEST (Biologia, Ecologia, Scienze della Terra) Unit of Biochemistry and Molecular Biotechnology, University of Calabria, Via P. Bucci 4C, 87036 Arcavacata di Rende, Italy.
Email: cesare.indiveri@unical.it

Funding information
Cure RTD, Grant/Award Number: Year 2019

Abstract

Riboflavin transporter deficiency 2 (RTD2) is a rare neurological disorder caused by mutations in the Solute carrier family 52 member 2 (Slc52a2) gene encoding human riboflavin transporter 2 (RFVT2). This transporter is ubiquitously expressed and mediates tissue distribution of riboflavin, a water-soluble vitamin that, after conversion into FMN and FAD, plays pivotal roles in carbohydrate, protein, and lipid metabolism. The 3D structure of RFVT2 has been constructed by homology modeling using three different templates that are equilibrative nucleoside transporter 1 (ENT1), Fucose: proton symporter, and glucose transporter type 5 (GLUT5). The structure has been validated by several approaches. All known point mutations of RFVT2, associated with RTD2, have been localized in the protein 3D model. Six of these mutations have been introduced in the recombinant protein for functional characterization. The mutants W31S, S52F, S128L, L312P, C325G, and M423V have been expressed in *E. coli*, purified, and reconstituted into proteoliposomes for transport assay. All the mutants showed impairment of function. The K_m for riboflavin of the mutants increased from about 3 to 9 times with respect to that of WT, whereas V_{max} was only marginally affected. This agrees with the improved outcome of most RTD2 patients after administration of high doses of riboflavin.

KEYWORDS

gene variants, proteoliposomes, rare diseases, riboflavin, structure–function relationship, transport proteins

1 | INTRODUCTION

Riboflavin, also known as vitamin B2, is a water-soluble compound that, after conversion into its biologically active forms, flavin mononucleotide (FMN) and flavin adenine dinucleotide (FAD), plays pivotal roles in biological redox reactions involved in carbohydrate, protein, and lipid metabolism, as well as in the metabolic conversion of vitamins B6 and B9 into their biologically active

Abbreviations: RTD, Riboflavin transporter deficiency; RFVT2, human riboflavin transporter 2; Slc52a2, Solute carrier family 52 member 2; ENT1, equilibrative nucleoside transporter 1; GLUT5, glucose transporter type 5; Slc52a1, Solute carrier family 52 member 1; RFVT1, human riboflavin transporter 1; RFT1, alias of human riboflavin transporter 1; RFT3, alias of human riboflavin transporter 2; SLC52A3, Solute carrier family 52 member 3; RFVT3, human riboflavin transporter 3; RFVT3, human riboflavin transporter 3; RFT2, alias of human riboflavin transporter 3.

forms.[1] Mammalians lost the ability to synthesize riboflavin despite the importance of flavin cofactor homeostasis for ensuring the functionality of hundreds of flavoenzymes. Indeed, the crucial role of riboflavin homeostasis is demonstrated by the occurrence of inherited diseases linked to defects of enzymes involved in its maintenance,[1–4] as well as by the fact that riboflavin deficiency also occurs in many diffused human pathologies such as diabetes mellitus, inflammatory bowel disease, and chronic alcoholism.[5–7] Riboflavin must be introduced through diet or derived from microbiota and enters the human body through intestinal absorption. The predominant role of carrier-mediated absorption of riboflavin in the small intestine has been postulated since 1966,[8] but the molecular identity of these systems remained cryptic for many years after due to the poor sequence similarity with the riboflavin transporter of yeast and bacteria. It was only in 2008 that the first riboflavin transporter, encoded by the Slc52a1 gene, was identified.[9] In total, three riboflavin transporters have now been identified with SLC52A1 corresponding to RFT1 or RFVT1; SLC52A2 corresponding to RFT3 or RFVT2; and SLC52A3 corresponding to RFT2 or RFVT3.[10] The fundamental role of these transporters for human health was demonstrated in 2010, when the link between RFVTs mutations and a neurodegenerative disorder known as Brown-Vialetto-Van Laere syndrome (BVVLS), was reported.[11,12] BVVLS was renamed to riboflavin transporter deficiency (RTD)[13] with pathogenic variants in the Slc52a2 and Slc52a3 genes corresponding to RTD type 2 and 3, respectively.[13,14] Both RTD types share several clinical manifestations, including sensorineural hearing loss, bulbar dysfunction, respiratory compromise, and muscle weakness.[13] The common symptomatology may be caused by partial overlapping of tissue expression of RVFT2 and RFVT3. RTD type 2 (OMIM #614707) can be distinguished by some specific symptoms such as abnormal gait/ataxia, optic atrophy and/or upper limb and axial predominant muscle weakness.[7,14] More than 50 SLC52A2 variants have been associated with this disorder.

In addition to clinical data, some experimental data on the functionality of the mutated RFVT2 have been reported.[15–18] Studies carried out using patient fibroblast or transient transfection of HEK293 cells demonstrated that riboflavin transport activity in mutant cells was dramatically reduced or abolished. The decreased activity reported for a number of these pathological variants was influenced by altered trafficking of the protein.[15] Subramanian et al.[18] demonstrated that introducing RFVT2 point mutations into human-derived brain U87 cells resulted in a reduction in protein stability/translation efficiency and impairment in transport function. A reliable system to obtain data on the actual transport function of pathological variants is the proteoliposome transport assay in which every single mutant can be tested. This in vitro system, which was successfully used to characterize the functional properties of the WT human RFVT2,[19,20] opened the possibility of investigating the functional alterations caused by natural point mutations.

In this study, we have performed a computational analysis on the transporters and their point mutations and characterized some of the mutants reported as clinically relevant based on their functional abnormalities.

2 | EXPERIMENTAL PROCEDURES

2.1 | Homology model generation

To select an appropriate template to build an accurate 3D model by homology modelling, the amino acid sequence of human RFVT2 was extracted from UNIPROT (Q9HAB3) and used as a query for BLAST against Protein Data Bank (PDB). Since no significant results were retrieved, a new search was performed using HHpred and Phyre2.[21,22] All the templates found had a sequence identity lower than 20%. For this reason, a multiple templates approach was attempted using MODELLER 9.24.[23] The selected templates were ENT1 (6ob7), the fucose: proton symporter (3o7p), and the rat GLUT5 (4ybq). These are in the outward-open conformation. After the generation of the multialignment, 100 models were constructed, then 16 of these were chosen based on a DOPE score range above the threshold of −0.465. The quality of the selected model was evaluated using PROCHECK, MOLPROB, VERIFY3D, ERRAT, and PROVE. The best scoring model was used for Docking analysis.

2.2 | Docking approach

Docking analysis was performed using AutoDock Vina v.1.1.2.[24] The grid box was generated on the whole protein to perform blind docking. The size of grid was set to 56 × 70 × 64 Å (x, y, and z) with spacing 1. Ligands were downloaded from PubChem in SDF format. The ligand was prepared and docked into the protein previously refined adding hydrogens and Kollman charges. Using Lamarkian Genetic Algorithm, 20 poses were carried out. The UCSF Chimera v.1.14 software[25] (Resource for Biocomputing, Visualization, and Informatics, University of California, San Francisco, California) was used for the molecular visualization.

2.3 | Site-directed mutagenesis and protein overexpression in *E. coli*

To over-express the recombinant RFVT2 proteins carrying the pathological mutations, the cDNA coding for RFVT2 (SLC52A2) optimized for *E. coli* codon usage, and cloned into the pH6EX3 plasmid, was used as the template to perform mutagenesis using Phusion Site-Directed Mutagenesis Kit by Thermo Scientific according to with miniature's instruction. WT and mutated cDNA of human RFVT2 were used to transform chemically competent *E. coli* Rosetta(DE3). After plate selection, a colony was inoculated in 100 ml of LB medium and cultured overnight at 37°C. The pre-culture was diluted 1:10 in fresh LB medium and when optical density reached 0.8, protein expression was induced adding 0.4 mM IPTG. After 4-h of incubation, cells were harvested and centrifuged. The bacterial pellet was suspended in a buffer containing NaCl 200 and 50 mM Hepes/Tris pH 7.5 and subjected to mild sonication at 4°C.[19,20] The expression of the RFVT2 mutants was tested by WB in comparison with WT protein. Figure S1A shows the expression of WT and mutants of hRFVT2.

2.4 | Purification of RFVT2 WT and mutants

Lysate was centrifuged at 12,000×*g* for 10 min at 4°C and the supernatant was discharged; The pellet was solubilized with 3 M urea, 0.8% Sarkosyl, 200 mM NaCl, 10 mM Tris/HCl pH 8.0 and centrifuged at 12,000×*g* for 10 min at 4°C. The supernatant was applied onto a His-select column pre-conditioned with 10 ml of a buffer containing 0.1% Sarkosyl, 200 mM NaCl, 10 mM Tris/HCl pH 8.0. After washing recombinant proteins (WT and mutants) were eluted with a buffer containing 0.1% C12E8, 200 mM NaCl, 10 mM Tris/HCl pH 8.0, and 50 mM imidazole.[20] Figure S1B shows the SDS-PAGE analysis of the purified proteins.

2.5 | Reconstitution of RFVT2 into liposomes and transport assay

A 0.4 ml aliquot of WT or mutants of FRVT2 (4 μg of purified protein) were mixed with 60 μl of 10% C12E8, 100 μl sonicated liposomes made with 10% egg yolk phospholipids, 70 μl of 200 mM Tris/HCl at 7.0 in a final volume of 700 μl. Protein concentration was assessed using the Bradford assay. Reconstitution was achieved by detergent removal by incubation with 0.55 g Amberlite XAD-4 under rotatory stirring at 22°C for 90 min. 550 μl of proteoliposomes were passed through a Sephadex G-75 column (0.7 cm diameter × 15 cm height) preequilibrated with a buffer containing 20 mM Tris/HCl at pH 7.0. The eluate was divided into aliquots of 100 μl. The transport activity was measured by adding 0.5 μM [^{3}H]Riboflavin to proteoliposomes and stopped at 5 min, which is within the initial linear range of the time course of uptake. To stop the assay, the reaction mix was passed through columns (0.6 cm diameter × 8 cm height) containing Sephadex G-75 to remove the radioactive substrate not taken up. The experimental values were corrected by subtracting the radioactivity taken up by control liposomes (not harboring the transporter in the membrane) from the radioactivity taken up by proteoliposomes.[19,20]

2.6 | Other methods

To verify RFVT2 overexpression in *E. coli*, 30 μg of total proteins from bacterial lysate was separated by SDS-PAGE on a 12% polyacrylamide gel and blotted to nitrocellulose membrane. The nitrocellulose membrane was treated with blocking buffer containing 3% BSA, 150 mM NaCl, 50 mM Tris–HCl pH 7.5, 0.05% Tween20 for 10 min, and then the anti-His peroxidase-conjugated antibody with a dilution of 1:40,000 was added to the buffer and incubated for 1 h at room temperature. Staining was performed using ECL select WB detection reagent from Amersham.

3 | RESULTS

3.1 | Construction and validation of RFVT2 homology model

Many of the single point mutations of SLC52A2 (Table S1) that have been reported are linked to the RTD syndrome. To predict possible structure/function relationships of these mutants in absence of a 3D structure of the protein, a homology model is mandatory. However, no suitable templates with identity higher than 20% with SLC52A2 are available. Thus, a strategy based on the use of several templates for constructing the model has been adopted. The best-scored template in terms of balance between identity (15%) and coverage (79%) corresponds to the human Equilibrative Nucleoside Transporter 1 (ENT1—6ob7).[26] This template does not cover the entire SLC52A2 sequence, hence two additional templates have been used: the Fucose: proton symporter (3o7p) from *E. coli*[27] and the rat glucose transporter GLUT5 (4ybq)[28] showing identities with RFTV2 of 11%

and 7% and coverages of 85% and 91%, respectively (Figure S2). The multiple sequence alignment among the RFVT2 and the templates was performed to allow model construction by using MODELLER 9.24. This alignment also takes into account hydropathy data and prediction of membrane protein topology(Figure S3).[29] It is important to report that the 3D templates are in the outward-open conformation of the transporters. Among 100 models generated by the MODELLER software, the best 16 models, showing Dope Scores above −0.465 (Figure 1A), were validated using several tools. After these analyses, the seventieth model was chosen as the best model. Figure 1B shows that 94% the amino acidic residues of RFVT2 model are in the Ramachandran Favoured region. The final model showed 11 transmembrane segments that line a large central cavity and two big loops located on the extracellular or the intracellular sides (Figure 2A,B).

To further assess the quality of the RFVT2 model, a blind docking analysis for Riboflavin, Lumiflavin, FMN, and FAD was performed. Indeed, from previously published results,[19,30] it is known that the riboflavin transport mediated by RFVT2 is inhibited by Lumiflavin and FMN but not by FAD. Using AutoDock Vina, the site of interaction for Riboflavin was predicted (Figure 3A). FMN interacts with the same site of Riboflavin (Figure 4B). Both these ligands show the same affinity (−8.3 kcal/mol) for the RFVT2. This correlates well with experimental results showing strong inhibition of the riboflavin transport in the presence of FMN. This suggests that FMN could act as a competitive inhibitor of riboflavin. Also, Lumiflavin, which lacks the ribitol moiety, shows comparable affinity (−8.0 kcal/mol) for the same site of RFVT2 (Figure 3C). Interestingly, the three molecules (riboflavin, FMN, and lumiflavin) mostly overlap in their location within the substrate-binding site, again in agreement with the riboflavin transport and the inhibition by FMN and lumiflavin previously observed (Figure 3D). On the contrary, FAD does not dock with the transporter in agreement with

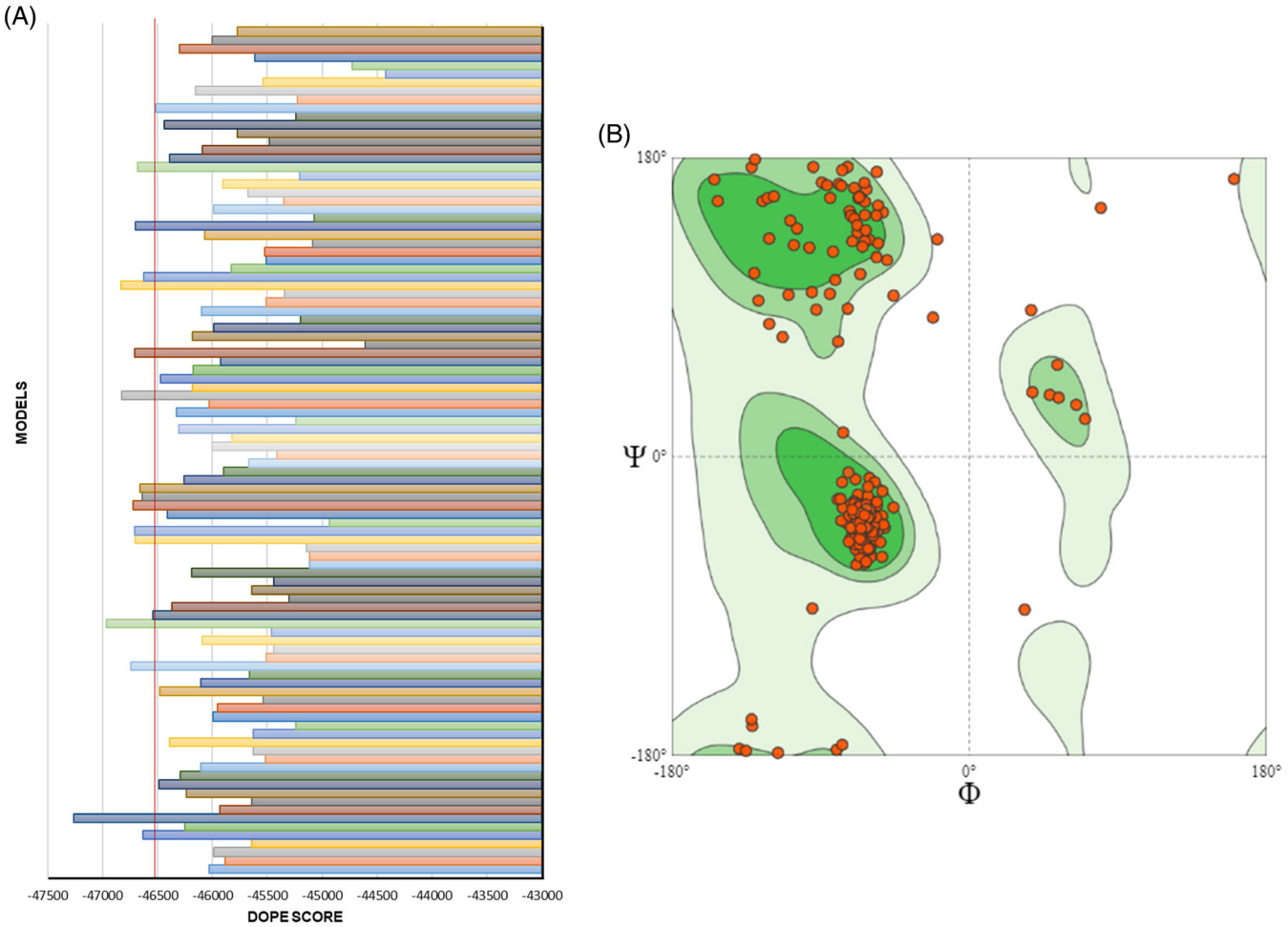

FIGURE 1 Evaluation of the quality of RFVT2 homology models. (A) DOPE score of the 100 models generated by MODELLER 9.24. The threshold of −0.465d is indicated as a red line. (B) Ramachandran plot of the best scoring model

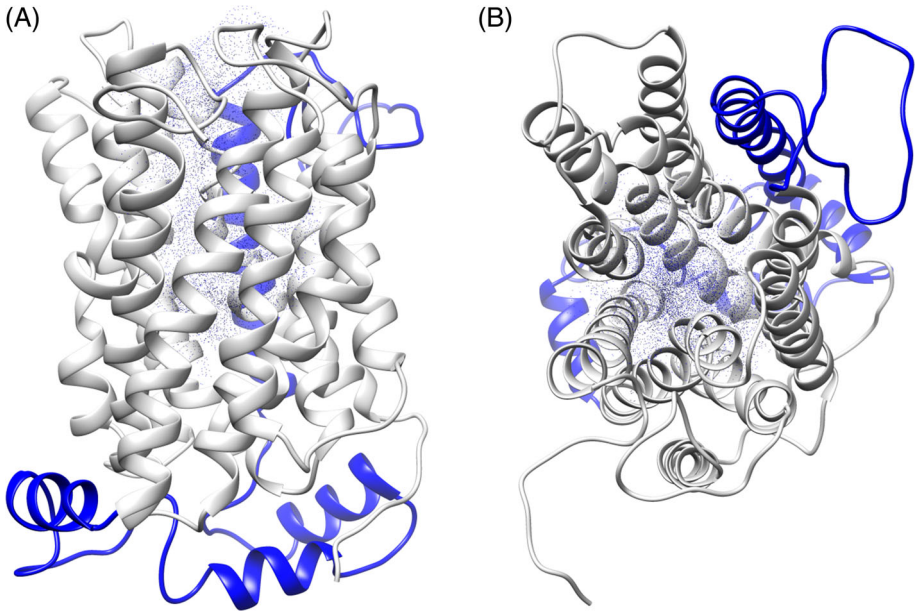

FIGURE 2 Structural model of RFVT2. (A) Lateral view and (B) top view of the ribbon diagram of the RFVT2. The 11 transmembrane α-helices are depicted as light gray ribbon. The region from the amino acid residues 173 to 276 is highlighted in blue. The homology model was constructed by MODELLER 9.24 using the crystallographic structures of ENT1, the Fucose:proton symporter, and GLUT5 as templates. Molecular graphics was performed with UCSF Chimera

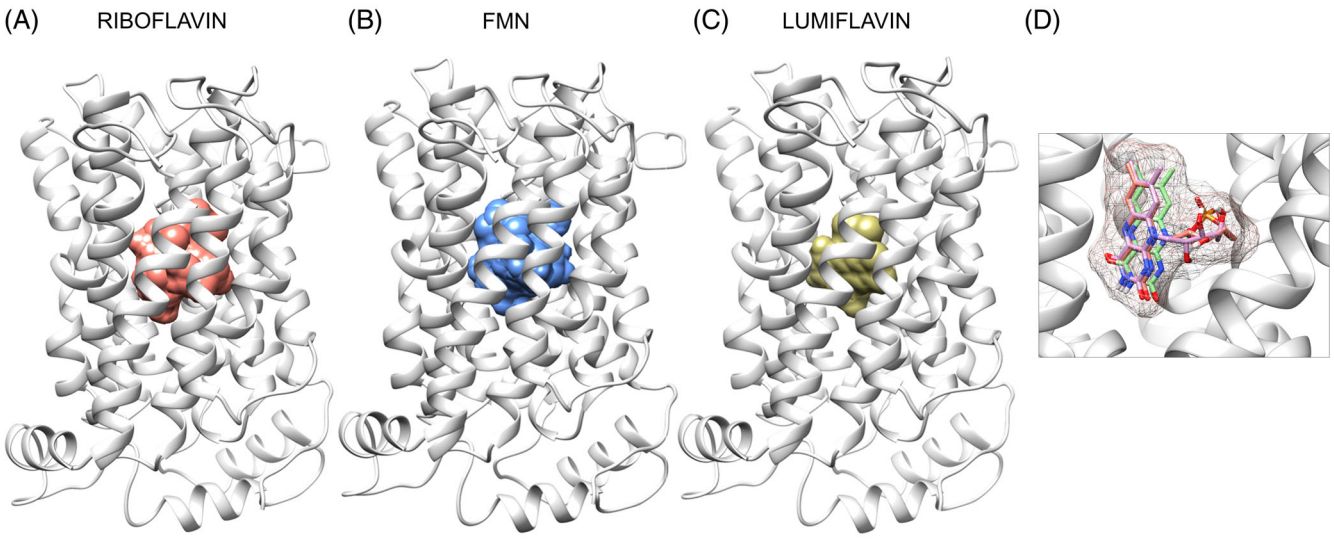

FIGURE 3 Docking analysis of the RFVT2. Docking analysis was performed using AutoDock Vina v.1.1.2. The homology model of RFVT2 in outward facing conformation was represented as light gray ribbon. The poses obtained by molecular docking analysis for (A) Riboflavin (in salmon), (B) FMN (blue) and (C) Lumiflavin (gold) are depicted as solid surface. (D) Enlarged view of the binding pocket of RFVT2. The three best poses of each substrate were superimposed and represented as sticks with mesh surface. The structure was visualized using Chimera 1.13.1 software

the lack of inhibition on riboflavin transport.[19] The good correlation between in silico and previous wet experiments suggests a sufficient degree of reliability of the generated RFVT2 model.

Starting from these results, the single point mutations of Table S1 have been located in the RFVT2 (Figure 4). The pathological mutants are distributed within the protein in various positions, from the central cavity to the hydrophobic interface with the membrane. The amino acid residues facing the central cavity may have a higher probability to interact with the substrate and hence their mutation may affect transport activity. On this basis, we choose to reproduce the pathological variant of some of these mutations in vitro, that is, W31S, L128S, C325G, and M425V (Figure 5). Moreover, we decided to also produce the mutant L312P. Indeed, the introduction of a Pro residue at the boundary between the eighth transmembrane segment and the loop facing toward the extramembrane side of the protein may result in the distortion of the structure(Figure 5).

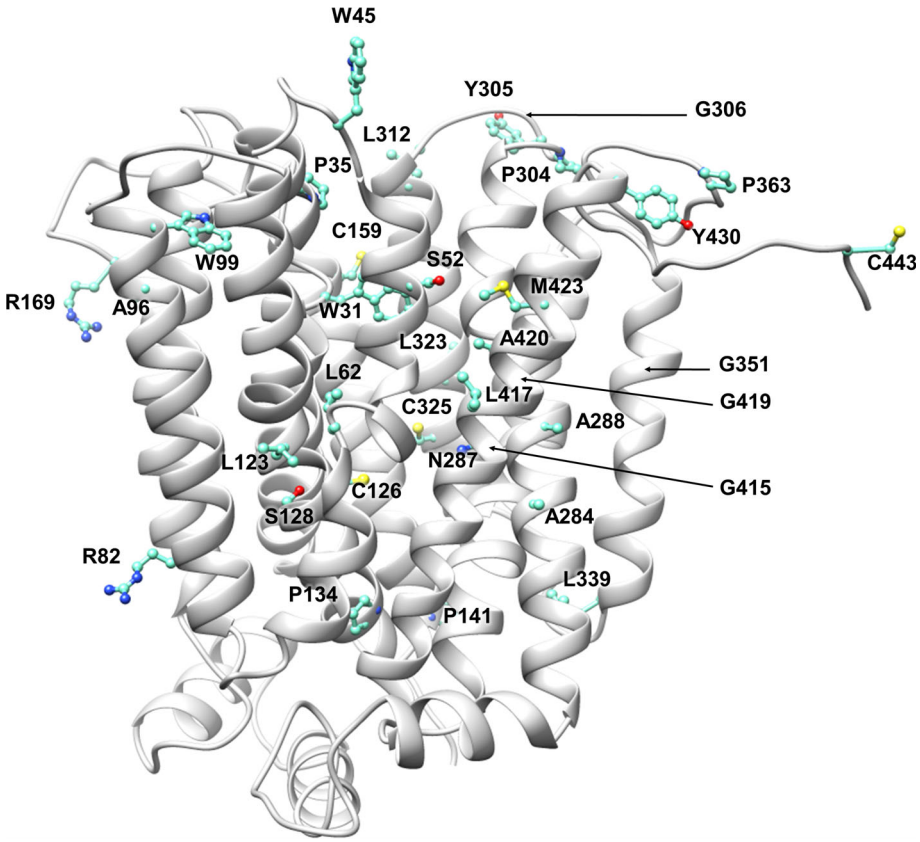

FIGURE 4 Position of RDT2-linked mutations in the RFVT2 homology model. Ribbon diagrams viewing the carrier from the lateral side. Side chain of amino acid residues which were found mutated in RTD2 patients were highlighted by ball and stick representation. Arrows indicate the position of glycine. The homology structural model has been represented using UCSF Chimera

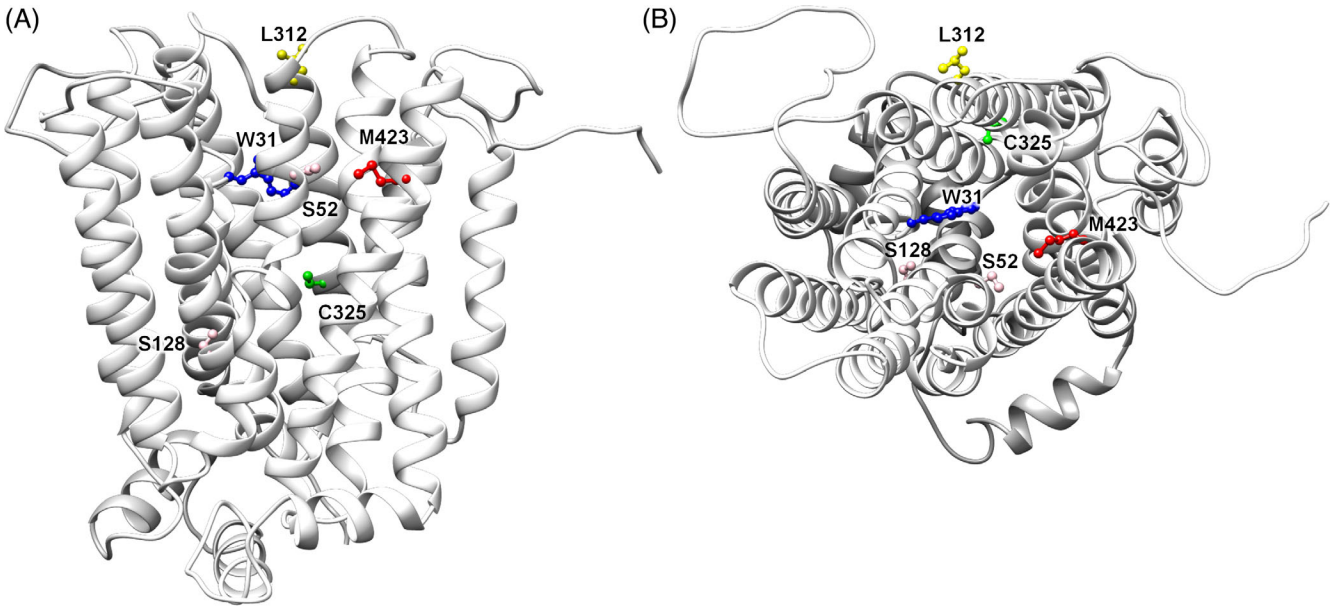

FIGURE 5 Position of RFVT2 mutants considered in this study. Ribbon diagrams viewing the carrier from the lateral side (A) or top view (B). Side chain of amino acid residues which were mutated in this study were highlighted by ball and stick representation. Arrows indicate the position of glycine. The homology structural model has been represented using UCSF Chimera

3.2 | Characterization of the transport activity of RFVT2 mutants

To test the effect of mutations on riboflavin transport activity, WT and mutants were expressed in *E. coli* and purified by nickel-chelating affinity chromatography. An equal amount of mutated and WT proteins was used to perform proteoliposomes reconstitution. Figure 6 shows that all the mutants were active, even if the activity of most mutants was impaired. Mutations that maximally

affect transport activity seem to be the S52F, L312P, and M423V.

Since all the mutants exhibited measurable transport activities, kinetic studies were feasible. Figure 7 shows the kinetic analysis for each mutant. Data were plotted according to the Michaelis–Menten equation. K_m and V_{max} values derived from the plots are indicated in the figure. The mutants S52F, M423V, L312P, and C325G showed strong variations of the K_m. Their values were 8.8, 7.6, 6.1, and 5.2 times higher than that of WT, respectively. Smaller variations of K_m, of about 3.2 and 2.9 fold, were observed for S128L and W31S mutants. The mutation-related variation of V_{max} was in the order of 15%. The only exception is mutant C325G that shows V_{max} value 1.8 fold higher than WT.

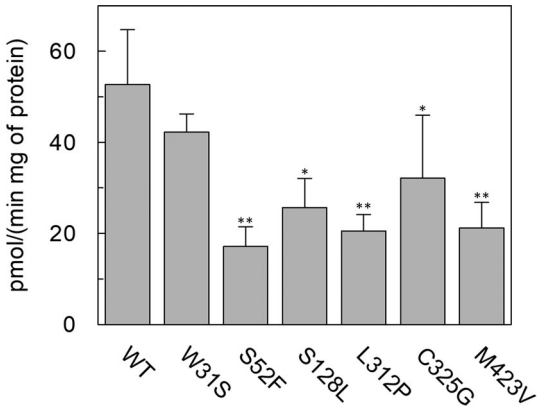

FIGURE 6 [^{3}H]Riboflavin uptake in proteoliposomes harbouring RFVT2 WT or mutants. Transport was started by the addition of 0.5 μM [^{3}H]Riboflavin to proteoliposomes and terminated after 5 min. The data represent means ± SD of three independent experiments. Statistics was performed using Student's *t*-test (*$p < 0.05$, **$p < 0.01$)

4 | DISCUSSION

To definitively approach the structure/function relationships of RFVT2, in view of its importance in human pathology, a suitable structural model was necessary. However, RFVT2, as well as the first and the third members of the SLC52 family, do not show appreciable identity with any other transporter from prokaryotes or eukaryotes so far structurally solved, which makes attempts of a straightforward construction of a homology model challenging. A more sophisticated strategy has been employed by optimizing the alignment of RFVT2 with three templates each exhibiting specific similarities with RFVT2. Bioinformatic analyses and correlation of docking of substrate and inhibitors with experimental data[19,30] concur in validating the suitability of the structural model. An analysis of the position of mutations reveals that a large percentage, roughly 56%, are in transmembrane segments, approximately 21% are at the boundary between the hydrophobic and the hydrophilic environment and 23% are in the hydrophilic loops. Interestingly no point mutations fall in the central region of the RFVT2 amino acid sequence (173–276), which include the large predicted

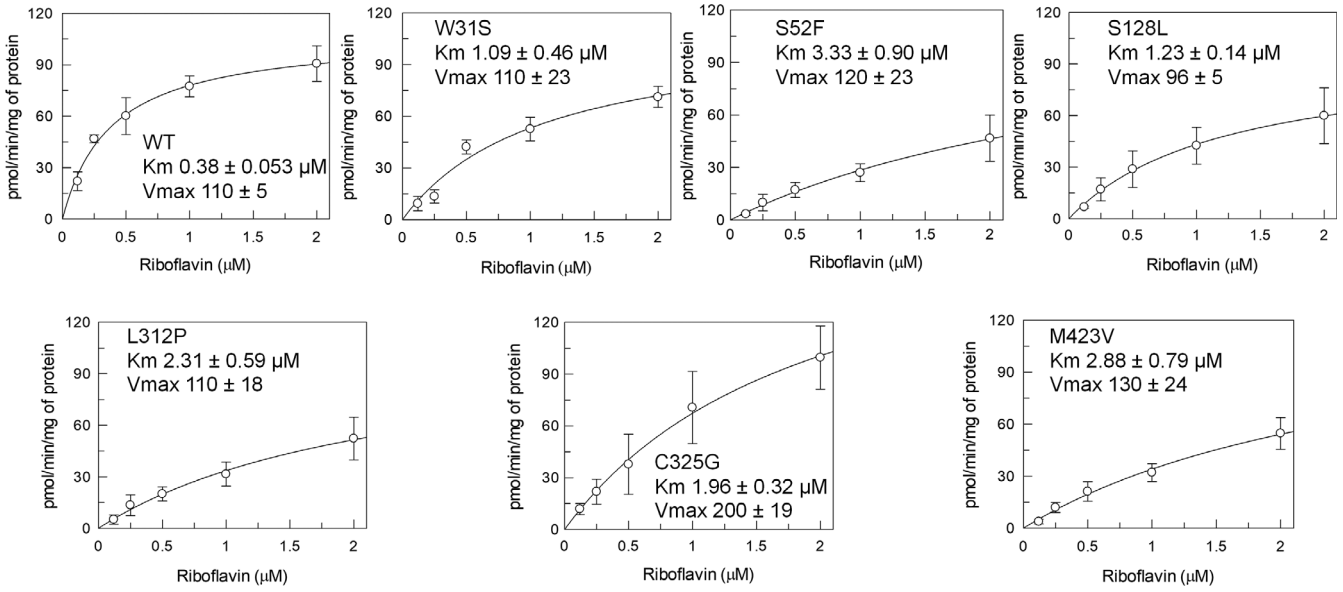

FIGURE 7 Kinetic characterization of RFVT2 mutants in comparison to WT. Transport was started by adding [^{3}H]Riboflavin at the indicated concentration to proteoliposomes reconstituted with WT or each of the mutants. The reaction time was 5 min. Data were plotted according to the Michaelis–Menten equation. The data represent the means ± SD of at last three independent experiments

```
SP|Q9HAB3|S52A2_HUMAN MAAPTPARPVLTHLLVALFGMGSWAAVNGIWVELPVVVKELPEGWSLPSYVSVLVALGNL 60
SP|B5MEV3|S52A2_RAT   MAAPPLGRLVLTHLLVALFGMGSWIAVNGIWVELPVVVKELPEGWSLPSYLSVLVALGNL 60
SP|Q9D8F3|S52A2_MOUSE MAAPPLGRLVLTHLLVALFGMGSWAAVNGIWVELPVVVKELPEGWSLPSYLSVLVALGNL 60
SP|Q863Y8|S52A2_PAPHA MAAPTLGHLVLTHLLVALLGMGSWAAVNGIWVELPVVVKHLPEGWSLPSYLSVVVALGNL 60
SP|Q863Y7|S52A2_PIG   MAAPTLARLVLTHLLVALFGMGSWAAINGIWVELPVVVKDLPEGWSLPSYLSVLVALGNL 60
                      ****  .: *********:***** *:************.**********:**:****** 

SP|Q9HAB3|S52A2_HUMAN GLLVVTLWRRLAPGKDEQVPIRVVQVLGMVGTALLASLWHHVAPVAGQLHSVAFLALAFV 120
SP|B5MEV3|S52A2_RAT   GLLLVTLWRRLAPGKSERIPIQVVQGLSIVGTGLLAPLWSNMALVAGQLHSVAFLTLAFV 120
SP|Q9D8F3|S52A2_MOUSE GLLLVTLWRRLARGKGEQVPIRVVQGLGIVGTGLLASLWNHVAPVAGKPYSVAFLTLAFV 120
SP|Q863Y8|S52A2_PAPHA GLLVVTLWRRLAPGKGERVPIQVVQVLSVVGTALLAPLWHHVAPVAGQLHSVAFLTLALV 120
SP|Q863Y7|S52A2_PIG   GLLVVTLWRRLAPGKGERAPIQVVQALSVVGTALLAPLWQHLTVMAGQVHSVAFLALTFV 120
                      ***:******** **.*: **:*** *.:***.*** ** ::: :**: :*****:*::* 

SP|Q9HAB3|S52A2_HUMAN LALACCASNVTFLPFLSHLPPRFLRSFFLGQGLSALLPCVLALVQGVGRLECPPAPINGT 180
SP|B5MEV3|S52A2_RAT   LALSCCASNVTFLPFLSHLPPPFLRSFFLGQGLSALLPCVLALAQGVGRLECLHVPANGT 180
SP|Q9D8F3|S52A2_MOUSE LALACCASNVTFLPFLSHLPPPFLRSFFLGQGLSALLPCVLALGQGVGRLECLHVPANRT 180
SP|Q863Y8|S52A2_PAPHA LALACCTSNVTFLPFLSHLPPPFLRSFFLGQGLSALLPCVLALVQGVGRLECSPAPTNGT 180
SP|Q863Y7|S52A2_PIG   LALACCASNVTYLPFLSRLPPPFLRSFFLGQGLSALLPCVLALGQGVGRLECPPAPANGT 180
                      ***:**:****:*****:*** ********************** ********  .* * *

SP|Q9HAB3|S52A2_HUMAN PGPP-----LDFLERFPASTFFWALTALLVASAAAFQGLLLLLPPPPSVPTGELGSGLQV 235
SP|B5MEV3|S52A2_RAT   TGPPIKVSPINFPERFSAGTFFWVLTALLGTSAAAFQGLLLLLPSPPPEA--TMGTGLRV 238
SP|Q9D8F3|S52A2_MOUSE TGPPIEVSPINFPERFSATTFFWVLTALLGTSAAAFQGLLLLLPSPTSEP--TTGTGLRV 238
SP|Q863Y8|S52A2_PAPHA SGPP-----LNFPERFPASTFYWALTALLVTSAAAFQGLLLLLPSLPSVTTGGAGPELPL 235
SP|Q863Y7|S52A2_PIG   PGPP-----LDFPERFSASAFFGALTALLVISAAAFQGLLLLLPSLVSIPTEGSGTGLRG 235
                       ***     ::* *** * :*: .*****  *************         *  *

SP|Q9HAB3|S52A2_HUMAN GAPGAEEEV---EESSPLQEPPSQAAGTTPGPDPKAYQLLSARSACLLGLLAATNALTNG 292
SP|B5MEV3|S52A2_RAT   ETPGTEEEE-EEEEASPLQEPPGQVASIVSSPDPKAHRLFSSRSACLLGLLAITNALTNG 297
SP|Q9D8F3|S52A2_MOUSE ETPGTEEEE-EEEEASPLQEPPGQVAGIVSSPDPKAHQLFSSRSACLLGLLAITNALTNG 297
SP|Q863Y8|S52A2_PAPHA GSPGAEEEEKEEEEALPLQEPPSQAAGTIPGPDPEAHQLFSAHGAFLLGLLAITSALTNG 295
SP|Q863Y7|S52A2_PIG   GAPGVEEEE--EEEASPLQEPPSQAAGNTPSPDPAAHRLLSARGACLLGLLATTSALTNG 293
                       :**.***    **: ******.*.*.   .*** *::*:*::.* ****** *.***** 

SP|Q9HAB3|S52A2_HUMAN VLPAVQSFSCLPYGRLAYHLAVVLGSAANPLACFLAMGVLCRSLAGLGGLSLLGVFCGGY 352
SP|B5MEV3|S52A2_RAT   VLPAVQSFSCLPYGRLAYHLAVVLGSSANPLACFLAMAVLCRSLAGLYGLCLLGMFFGTY 357
SP|Q9D8F3|S52A2_MOUSE VLPAVQSFSCLPYGRLAYHLAVVLGSCANPLACFLAMAVLCRSLAGLCGLSLLGMLLGSY 357
SP|Q863Y8|S52A2_PAPHA VLPAVQSFSCLPYGRLAYHLAVVLGSAANPLACFLAMGVLCRSLAGLVGLSLLGMLFGAY 355
SP|Q863Y7|S52A2_PIG   VLPAVQSYSSLPYGRLAYHLAVVLGSASNPLACFLAMGILCRSLAGLGGLSLLGTLFGAY 353
                      *******:*.****************.:*********.:******** **.*** : * *

SP|Q9HAB3|S52A2_HUMAN LMALAVLSPCPPLVGTSAGVVLVVLSWVLCLGVFSYVKVAASSLLHGGGRPALLAAGVAI 412
SP|B5MEV3|S52A2_RAT   LMTLAVLSPCPPLVGTSAGVVLVVLSWVLCAGVFSYIKVATSSMLHSGGRPALLAAGVAI 417
SP|Q9D8F3|S52A2_MOUSE LMTLAALSPCPPLVGTSAGVVLVVLSWVLCAGTFSYIKVAISSMLHSGGRPALLAAGVAI 417
SP|Q863Y8|S52A2_PAPHA LMVLAILSPCPPLVGTTAGVVLVVLSWVLCLCVFSYVKVAASSLLHGGGRPALLAAGVAI 415
SP|Q863Y7|S52A2_PIG   LMALAILSPCPPLVGTSAGMVLVVVLWALCLGVFSYVKVATSSLLHGGGPPALLAAGVAI 413
                      **.** **********:**:****: *.**  .***:*** **:**.** **********

SP|Q9HAB3|S52A2_HUMAN QVGSLLGAVAMFPPTSIYHVFHSRKDCADPCDS 445
SP|B5MEV3|S52A2_RAT   QVGSLLGAIAMFPPTSVYPVFRSGEDCVDQCGP 450
SP|Q9D8F3|S52A2_MOUSE QVGSLLGAVAMFPPTSIYRVFRSGKDCVDQCGL 450
SP|Q863Y8|S52A2_PAPHA QMGSLLGAGTMFPPTSIYHVFQSRKDCVDPCGP 448
SP|Q863Y7|S52A2_PIG   QVGSLLGAVTMFPPTSIYRVFQSRKDCVDPCEP 446
                      *:******* :******:* **:* :**.* *
```

FIGURE 8 Alignment of RFVT2 amino acid sequences from different species. RFVT2 sequences were aligned using the Clustal Omega software. Identities are indicated by asterisks and conservative or highly conservative substitutions are indicated by dots or colons, respectively. RFVT2 mutants considered in this study are highlighted in yellow; the less conserved region corresponding to the large intracellular loop of RFVT2 is displayed in gray

extracellular loop, the sixth transmembrane segment, and the large predicted intracellular loop (Figure 2). This region is less conserved among the different species with respect to the other regions (Figure 8). This composite segment probably has species-specific roles in the protein function. Based on the structural model, the transmembrane α-helix 6 included in this segment, faces the membrane, not the substrate binding site in the protein core. This segment may also be involved in the interaction with another protein subunit to form oligomers. Indeed, one of the templates used for the 3D modelling, namely ENT1, forms dimeric structures.[26,31] Moreover, Figure S1A shows, in some cases the presence of a faint band at a molecular mass about double that of the protein monomer, still in favor of the presence of formation of a dimeric structure that is maintained also after treatment of the samples with the SDS for gel running. However, additional investigations are in progress using biophysical methods to ascertain this possibility. Of interest, Ciccolella et al.[16] reported a reduction of both RFVT1 and RFVT2 protein without a change in SLC52A1 mRNA expression in fibroblasts from a patient with RTD type 2, suggesting that RFVT2 may also be involved in the formation of heterodimers with the RFVT1. In agreement with a specific role of the loop–helix–loop region, one of the hydrophilic large loops, which contains many acidic residues, could be a site of regulation by Ca^{++}, as previously hypothesized.[19]

It must be stressed that not only the position of the mutated residues but also the replacing amino acid residues will contribute to the final effect on the transport function. Most of the residues that we have selected for performing site-directed mutagenesis and transport analysis surround the substrate binding site. Indeed, their substitutions cause a large increase in K_m and a substantial decrease in affinity towards riboflavin. We also selected the mutant L312P in which the WT amino acid is substituted by a relatively different residue. This mutation is far from the substrate binding pocket but still results in a large increase of K_m. In this case, the substitution of the branched chain of Leu with the cyclic residue of Pro may cause a distortion of the structure at the boundary between the membrane and the aqueous environment, destabilizing the interaction of the transporter with the membrane and/or impairment of the substrate access to the internal site. Among the residues tested for mutagenesis, W31 appears to be less crucial with the smallest increase in K_m. Therefore, W31 does not appear critical for the transport process, but it may be temporarily involved in riboflavin access to the binding site. However, given that most people identified with RTD have combinations of two different mutations occurring in the different alleles, it is not possible to precisely link the alteration of the protein function to the severity of the syndrome. Riboflavin supplementation has been shown to ameliorate the progression of RTD and can be potentially life-saving.[15] Outcomes following treatment have included improvement in muscle strength, ataxia, respiratory function, visual acuity, and hearing in many patients or stabilization of function.[13–15] Untreated patients typically experience gradual deterioration, often leading to death due to respiratory insufficiency. These patient outcomes are in agreement with the finding that the mutations cause a strong decrease of affinity for riboflavin while the maximal transport rate, that is, the transport rate at very high riboflavin concentration, is not affected by the mutations. The K_m impairment is deleterious for the patients in view of the low concentration of circulating Rf which is around 10 nM, that is, much lower than the WT K_m. However, in some cases, the kinetic impairment may not fully correlate with the patient outcomes. Indeed, some mutations may also alter the stability of the mRNA/protein or the trafficking to the membrane, resulting in a muted patient response to riboflavin supplementation despite only minor or no kinetic impairment to the RFVT protein. Mice knocked out of RFVT2 failed to be generated since Slc52a2 gene deficiency results in early embryonic lethality. This is in line with the described expression of RFVT2 in the fetal brain, while RFVT1 is not present in the brain, but in the placenta. Several SLC52A2 mutations reported in RTD patients have been reading frame interruption by a premature stop codon expected to result in a non-functional protein.[32] However, these non-functional protein mutations have never been reported in a homozygous state in patients suggesting at least one partially functioning protein is a prerequisite for birth.

Interestingly, the data from bioinformatics correlates well with the mutant transport assay indicating that the sole bioinformatics, which is much easier to perform than the transport assay analysis, might represent a useful predictive/screening tool. The suitability of bioinformatics could be increased by a more refined homology model that may be constructed if better templates will be available.

CONFLICTS OF INTEREST

The authors declare no conflict of interest.

FUNDING

This research was funded by a grant from Cure RTD (Year 2019) http://curertd.org/news/new/.

AUTHOR CONTRIBUTIONS

Lara Console performed the experiments, the bioinformatics, and manuscript writing. Jessica Cosco performed

the bioinformatics. Maria Tolomeo contributed to experiments on protein production and manuscript writing. Keith Massey contributed to data interpretation and manuscript writing. Maria Barile and Cesare Indiveri conceived the study and wrote the manuscript. All authors read and approved the submitted version.

ORCID

Cesare Indiveri https://orcid.org/0000-0001-9818-6621

REFERENCES

1. Barile M, Giancaspero TA, Leone P, Galluccio M, Indiveri C. Riboflavin transport and metabolism in humans. J Inherit Metab Dis. 2016;39:545–557.
2. Bafunno V, Giancaspero TA, Brizio C, et al. Riboflavin uptake and FAD synthesis in *Saccharomyces cerevisiae* mitochondria: involvement of the Flx1p carrier in FAD export. J Biol Chem. 2004;279:95–102.
3. Olsen RKJ, Konarikova E, Giancaspero TA, et al. Riboflavin-responsive and -non-responsive mutations in FAD synthase cause multiple acyl-CoA dehydrogenase and combined respiratory-chain deficiency. Am J Hum Genet. 2016;98:1130–1145.
4. Gianazza E, Eberini I, Sensi C, Barile M, Vergani L, et al. Energy matters: mitochondrial proteomics for biomedicine. Proteomics. 2011;11:657–674.
5. Fernandez-Banares F, Abad-Lacruz A, Xiol X, et al. Vitamin status in patients with inflammatory bowel disease. Am J Gastroenterol. 1989;84:744–748.
6. Rosenthal WS, Adham NF, Lopez R, Cooperman JM. Riboflavin deficiency in complicated chronic alcoholism. Am J Clin Nutr. 1973;26:858–860.
7. Mosegaard S, Dipace G, Bross P, Carlsen J, Gregersen N, Olsen RKJ. Riboflavin deficiency: implications for general human health and inborn errors of metabolism. Int J Mol Sci. 2020;21:3847–3872.
8. Levy G, Jusko WJ. Factors affecting the absorption of riboflavin in man. J Pharm Sci. 1966;55:285–289.
9. Yonezawa A, Masuda S, Katsura T, Inui K. Identification and functional characterization of a novel human and rat riboflavin transporter, RFT1. Am J Physiol Cell Physiol. 2008;295:C632–C641.
10. Yonezawa A, Inui K. Novel riboflavin transporter family RFVT/SLC52: identification, nomenclature, functional characterization and genetic diseases of RFVT/SLC52. Mol Aspects Med. 2013;34:693–701.
11. Green P, Wiseman M, Crow YJ, et al. Brown-Vialetto-Van Laere syndrome, a ponto-bulbar palsy with deafness, is caused by mutations in c20orf54. Am J Hum Genet. 2010;86:485–489.
12. Bosch AM, Abeling NG, Ijlst L, et al. Brown-Vialetto-Van Laere and Fazio Londe syndrome is associated with a riboflavin transporter defect mimicking mild MADD: a new inborn error of metabolism with potential treatment. J Inherit Metab Dis. 2011;34:159–164.
13. O'Callaghan B, Bosch AM, Houlden H. An update on the genetics, clinical presentation, and pathomechanisms of human riboflavin transporter deficiency. J Inherit Metab Dis. 2019;42:598–607.
14. Amir F, Atzinger C, Massey K, Greinwald J, Hunter LL, Kettler M. The clinical journey of patients with riboflavin transporter deficiency type 2. J Child Neurol. 2020;35:283–290.
15. Foley AR, Menezes MP, Pandraud A, et al. Treatable childhood neuronopathy caused by mutations in riboflavin transporter RFVT2. Brain. 2014;137:44–56.
16. Ciccolella M, Corti S, Catteruccia M, et al. Riboflavin transporter 3 involvement in infantile Brown-Vialetto-Van Laere disease: two novel mutations. J Med Genet. 2013;50:104–107.
17. Haack TB, Makowski C, Yao Y, et al. Impaired riboflavin transport due to missense mutations in SLC52A2 causes Brown-Vialetto-Van Laere syndrome. J Inherit Metab Dis. 2012;35:943–948.
18. Subramanian VS, Kapadia R, Ghosal A, Said HM. Identification of residues/sequences in the human riboflavin transporter-2 that is important for function and cell biology. Nutr Metab (Lond). 2015;12:13.
19. Console L, Tolomeo M, Colella M, Barile M, Indiveri C. Reconstitution in proteoliposomes of the recombinant human riboflavin transporter 2 (SLC52A2) overexpressed in *E. coli*. Int J Mol Sci. 2019;20:4416–4428.
20. Console L, Tolomeo M, Indiveri C. Functional study of the human riboflavin transporter 2 using proteoliposomes system. Methods Mol Biol. 2021;2280:45–54.
21. Gabler F, Nam SZ, Till S, et al. Protein sequence analysis using the MPI bioinformatics toolkit. Curr Protoc Bioinformatics. 2020;72:e108.
22. Kelley LA, Mezulis S, Yates CM, Wass MN, Sternberg MJ. The Phyre2 web portal for protein modeling, prediction and analysis. Nat Protoc. 2015;10:845–858.
23. Webb B, Sali A. Comparative protein structure modeling using MODELLER. Curr Protoc Bioinform. 2016;54:5.6.1–5.6.37.
24. Trott O, Olson AJ. AutoDock Vina: improving the speed and accuracy of docking with a new scoring function, efficient optimization, and multithreading. J Comput Chem. 2010;31:455–461.
25. Pettersen EF, Goddard TD, Huang CC, et al. UCSF chimera: a visualization system for exploratory research and analysis. J Comput Chem. 2004;25:1605–1612.
26. Wright NJ, Lee SY. Structures of human ENT1 in complex with adenosine reuptake inhibitors. Nat Struct Mol Biol. 2019;26:599–606.
27. Dang S, Sun L, Huang Y, Lu F, Liu Y, et al. Structure of a fucose transporter in an outward-open conformation. Nature. 2010;467:734–738.
28. Nomura N, Verdon G, Kang HJ, et al. Structure and mechanism of the mammalian fructose transporter GLUT5. Nature. 2015;526:397–401.
29. Tsirigos KD, Peters C, Shu N, Kall L, Elofsson A. The TOPCONS web server for consensus prediction of membrane protein topology and signal peptides. Nucleic Acids Res. 2015;43:W401–W407.
30. Yao Y, Yonezawa A, Yoshimatsu H, Masuda S, Katsura T, Inui K-I. Identification and comparative functional characterization of a new human riboflavin transporter hRFT3 expressed in the brain. J Nutr. 2010;140:1220–1226.
31. Bicket A, Coe IR. N-linked glycosylation of N48 is required for equilibrative nucleoside transporter 1 (ENT1) function. Biosci Rep. 2016;36:e00376.

32. Petrovski S, Shashi V, Petrou S, et al. Exome sequencing results in successful riboflavin treatment of a rapidly progressive neurological condition. Cold Spring Harb Mol Case Stud. 2015;1: a000257.

SUPPORTING INFORMATION

Additional supporting information may be found in the online version of the article at the publisher's website.

How to cite this article: Console L, Tolomeo M, Cosco J, Massey K, Barile M, Indiveri C. Impact of natural mutations on the riboflavin transporter 2 and their relevance to human riboflavin transporter deficiency 2. IUBMB Life. 2021;1–11. https://doi.org/10.1002/iub.2541